www.icgst.com

Automatic Recognition of Lesion-like Regions in Black Skin Medical Images

G. Azehoun-Pazou, K. Assogba
LETIA, Polytechnic School of Abomey-Calavi, 01 BP 2009, Abomey-Calavi, Rep. Benin
geraud.pazou@gmail.com, mkokouassogba@yahoo.fr

Abstract
This paper presents a study made to automatically recognize lesion-like regions in black skin medical images. Skin lesions have consistently had one of the most rapidly increasing incidences of all cancers. Early diagnosis is particularly important but it is a challenging task, especially for black populations. Moreover, black skin specialists are often limited to the use of classic macroscopic images for diagnosis purpose. All these difficulties are related to black skin pigmentation level and the small visual differences between lesion parts and healthy ones.
We propose here a computerized method which identifies automatically lesion regions with more accuracy and efficiency. It works like an automaton that traverse lesion images and automatically classifies healthy regions from lesions regions. The designed classifier is a Multi-Layer Perceptron Artificial Neural Network (MLP-ANN) trained with color and texture features. We made many combinations of features and varied the number of neurons in hidden layer, in order to obtain best performances. Nine features (six of texture and three of color) have been retained to train the network. The achieved classification performance is 97.2% in both training, validation and testing set. [1]

Keywords: *Medical images, Black skin, Neural Network, Lesion recognition, Texture features.*

Nomenclature

ANN	Artificial Neural Network
CAD	Computer Aided Diagnosis
MLP	Multi-Layer Perceptron
MLP-ANN	Multi-Layer Perceptron type Artificial Neural Network
CADS	Computer Aided Diagnosis System
PPV	Positive Predictive Value or Precision
NPV	Negative Predictive Value
TPR	True Positive rate or Sensitivity
SPC	Specificity or True Negative Rate
FPR	False Positive Rate
ACC	Accuracy
FP	False Positive
FN	False negative
TP	True Positive
TN	True Negative

1. Introduction
Dermatology is one of the fields where medical images have been used for years, since their potential benefits had been revealed in 1992 by Stoecker and Moss [1]. However, many parameters such as: type and quality of images, noise, or acquisition techniques influence image processing. About that, black skin images are certainly one for which difficulties occur most. In fact, while several studies proved the effectiveness of dermoscopic images based diagnosis [2-5], dermoscopy is ineffective in black skin and then unusable by black skin specialists. Therefore, these specialists are limited to the use of standard digital cameras as acquisition devices. Once images are acquired, major difficulties appear regarding their processing.
Indeed, in black skin, there is the presence of pigment throughout the basal layer of epidermis [6]. Therefore, the approach with black population is quite different, even if diagnostic procedure is generally the same, regardless of skin color [7]. So, it is important to make research in the direction of setting up Computer Aided Diagnosis (CAD) systems specific to black skin. In this context, we proposed in a previous paper, a method to analyze black skin macroscopic medical images. In that work, we focused on preprocessing and segmentation using a combination of mathematical morphology and edge detection [8]. The method improved edge detection but had also shown its limits. So, further studies deserved to be undertaken in order to develop a more efficient system.
With the significant advances occurred during recent years in the field of computer science and artificial intelligence, medical images processing has become more reliable and accurate [9]. Some good applications can be found in [10], [11] [12] and [13]. Artificial Neural Networks (ANNs) in particular, have been use to solve many image processing problems, as reported in [14], [15]

[1] This study has been implemented on Matlab Neural Network Toolbox software at LETIA lab. University of Abomey-Calavi in Republic of Benin

and [16]. Among them, we can enumerate: applications of ANNs in pre-processing step [17-19]; ANNs trained to perform segmentation task [20-22]. ANNs have also been used in medical diagnosis as main stage of a CADS [23]. Despite these advances, there exist very few studies on the subject of black skin, as regards the development of CADS. The typical pipeline adopted for automated skin lesion diagnosis is: image acquisition, artifact detection, lesion segmentation, feature extraction and classification [24]. In this paper, we propose a neural network based classifier acting in the artifact detection stage. It has been trained with color and texture features and works like an automaton that traverse black skin lesion images and automatically differentiates healthy regions from lesions regions.

The remainder of the paper is organized as follows: Section (2) discusses the theory about feedforward type neural networks; Section (3) emphasizes on the material and the methods used in this work; In Section (4) we present the results and make some discussions and finally, we conclude in Section (5).

2. Theory

An Artificial Neural Network is a computational system inspired by the structure, the processing method and the learning ability of a biological brain. It is characterized by a large number of very simple neuron-like processing elements, a large number of weighted connections (links) between these elements and a distributed representation of knowledge over the connections [25]. Knowledge is acquired by the network through a learning process [26]. ANNs' expansion started in 1943 when McCulloch and Pitts proved that neuron can have two states and that those states could be dependent on some threshold value [27]. Since then, ANNs have been widely used in research because they can model highly non-linear systems in which the relationship among the variables is unknown or very complex [28]. A review of various classes of neural networks can be found in [29] and [30]. Multilayer perceptrons (MLPs) are the most popular type of neural networks in use today. They belong to a general class of structures called feedforward neural networks, a basic type of neural network capable of approximating generic classes of functions, including continuous and integrable functions [31].

MLP Structure: In MLP structure, neurons are grouped into layers. The first and last layers are called input and output layers respectively, because they represent inputs and outputs of the overall network. The remaining layers are called hidden layers. Typically, an MLP neural network consists of an input layer, one or more hidden layers, and an output layer, as shown in Figure 1.

Mathematical background: Suppose the total number of layers is L. The 1^{st} layer is the input layer, the ℓ^{th} layer is the output layer, and layers 2 to $L-1$ are hidden layers. Let the number of neurons in ℓ^{th} layer be N_ℓ, $\ell = 1,2,...,\mathrm{L}$ and w_{ij}^{ℓ} represent the weight of the link between j^{th} neuron of $\ell-1^{th}$ layer and i^{th} neuron of ℓ^{th} layer, $1 \leq j \leq N_{\ell-1}$, *and* $1 \leq i \leq N_\ell$. Let x_i represent the i^{th} external input to the MLP, and z_i^{ℓ} be the output of i^{th} neuron of ℓ^{th} layer. An extra weight parameter w_{i0}^{ℓ} is introduced for each neuron, representing the bias for i^{th} neuron of ℓ^{th} layer. As such, $\boldsymbol{w}$ of MLP includes w_{ij}^{ℓ}, $j=0,1,..., N_{\ell-1}$, $i=1,2,..., N_\ell$, $\ell=2,3,...,L$. $\boldsymbol{w}$ expression is given by equation (1):

$$w = \left[w_{10}^2 \; w_{11}^2 \; w_{12}^2 \; ... \; w_{N_L N_{L-1}}^L \right]^T \qquad (1)$$

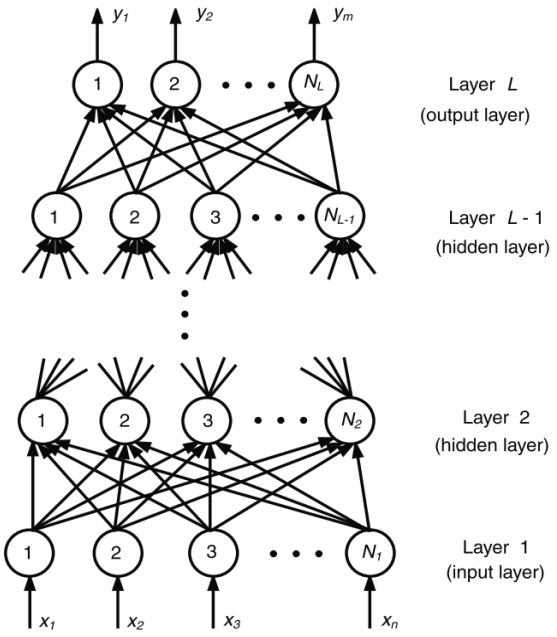

Figure 1. Multilayer perceptron (MLP) Neural Network structure

In a neural network, each neuron with the exception of neurons at the input layer receives and processes stimuli (inputs) from other neurons. The processed information is available at the output end of the neuron. A neuron of the ℓ^{th} layer receives stimuli from neurons of $\ell-1^{th}$ layer, that is: $h_\ell^{\ell\text{-}1}, h_\ell^{\ell\text{-}2}, ..., h_{\mathrm{N}_{\ell\text{-}1}}^{\ell\text{-}1}$. Each input is multiplied by the corresponding weight parameter, and resulting products are added to produce a weighted sum γ_i^{ℓ} (cf. equation 3). This weighted sum is passed through a neuron activation function σ to produce the final output h_i^{ℓ} of the neuron (cf. equation 2). This output represents the hypothesis (or assumption) of the neuron, and it can become the stimulus for neurons in the next layer:

$$h_i^{\ell} = \sigma(\gamma_i^{\ell}) \quad (2); \qquad \gamma_i^{\ell} = \sum_{j=0}^{N_{\ell-1}} w_{ij}^{\ell} h_j^{\ell-1} \quad (3)$$

Learning process: The purpose of ANN is to learn to recognize patterns in data. Once the neural network has been trained on samples data, it can make predictions by detecting similar patterns in future data. The process by which MLP neural network achieves learning or training is a two steps: feedforward and backpropagation.

In the feedforward process, the external inputs are first fed to the input neurons 1st layer, the outputs from the input neurons are fed to the hidden neurons of the 2nd layer, and so on, and finally the outputs of $L-1^{th}$ layer are

fed to the output neurons L^{th} layer. The difference between the resulting outputs and the expected ones is calculated to get the error. In backpropagation, errors that result from previous step are propagated back through the system, causing the system to adjust the connection weights. The training begins with random weights and the goal is to adjust them until the error is minimal. This is achieved by minimizing the objective function E of equation (4):

$$E = \frac{1}{2}\sum_{i=1}^{m}(h_i^L - y_i)^2 \qquad (4)$$

More details about ANN learning process is available in [26].

3. Material and methods

Material: We implemented our programs and algorithms with MATLAB, Version 8.4 (R2014b). We designed, implemented and trained the network with the MATLAB neural network toolbox. Our data set includes 40 medical images which were taken in same conditions (cf. Table I).

Table I. Images Database Composition

Types of Images	Number
Erythema lesion	17
Tuberous Sclerosis Complex (TSC) lesion	6
Purpura lesion	5
Seborrheic Keratosis lesion	7
Eczema lesion	5
Images showing black people skin	20

These images were taken with a HD digital camera in the Dermatology service of the Hubert K. Maga University Hospital of Cotonou. Figure 2 shows samples from each type of skin lesion.

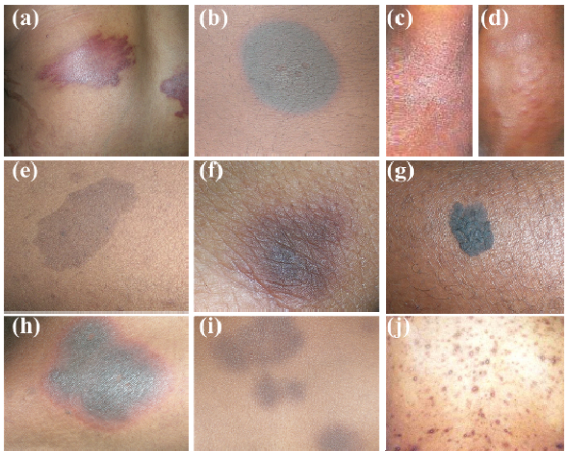

Figure 2. Some black skin lesions of our image database (a: Purpura lesion; c - j : Eczema lesion; e: TSC lesion; g: Seborrheic Keratosis; b - d - f - h - i : different types of Erythema)

We also downloaded images showing black people skin, from different online databases. From all these images, we extracted blocks of pixels of size 3x3, thanks to a program. Each block represents an example of the dataset (see figure 3 for extraction procedure). At the end, we obtained about 800.000 learning examples that we divided into learning, validation and test sets, in the respective proportions of 60%, 20% and 20%.

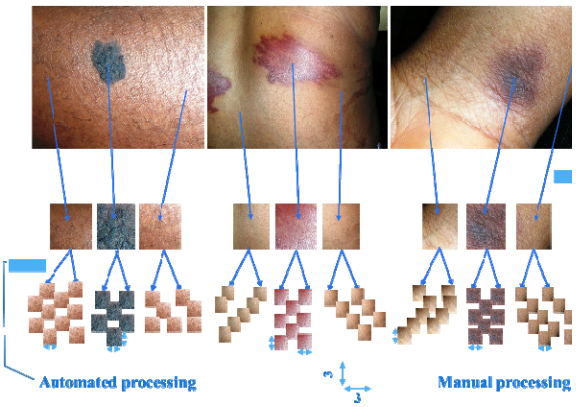

Figure 3. Regions extraction to blocks of pixels constitution

Methods: Normal skin regions are homogenous connected groups of pixels. So, color and texture information can be used to describe them. Fifteen features were identified to train the NN, but nine were finally retained. So the designed network has nine neurons in input layer and one in output layer. We varied the number of neurons in the hidden layer until we get the best performances. The input layer neurons correspond to features calculated for each example (3x3 pixel block). There are three color descriptors (one for each RGB color channel) and six texture descriptors.

Color features: We calculate the mean intensity value for each of the R, G and B channels (M_R, M_G and M_B) with formula (5).

- for each block X (3,3),

$$M_k = \frac{1}{9}\sum_{i=1}^{9} x(i) \quad (5), \qquad k = \{R, G, B\}$$

Texture features: The retained texture features are: uniformity, standard deviation, skewness, kurtosis, smoothness, and entropy. They were chosen for their simplicity and efficiency. Let z_i represent the value of a pixel $x(i)$; features are defined as follows:

- Uniformity: it is maximum when all gray levels are equal (maximally uniform).

$$U = \sum_{i=1}^{l} p^2(z_i) \qquad (6)$$

- Standard deviation: measure of average contrast.

$$\sigma = \sum_{i=1}^{l}(z_i - m)^2 p(z_i) \qquad (7)$$

- Skewness: it is the measure of the asymmetry of the intensity values around the mean intensity.

$$s = \sum_{i=1}^{l}(z_i - m)^3 p(z_i) \qquad (8)$$

- Smoothness: its value is 0 for regions of constant intensity and approaches 1 for regions with large excursions in the values of its intensity levels.

$$r = 1 - \frac{1}{1+\sigma^2} \quad (9)$$

- Kurtosis: it is the measure of how outlier-prone a distribution is.

$$s = \sum_{i=1}^{l} (z_i - m)^4 p(z_i) \quad (10)$$

- Entropy: a measure of randomness.

$$e = -\sum_{i=1}^{l} p(z_i) \log_2 p(z_i) \quad (11)$$

With:

- l the number of possible intensity levels;
- z_i a random value of pixel intensity;
- $p(z_i)$ the histogram of intensity levels in a region around z_i;
- and m the average intensity defined by:

$$m = \sum_{i=1}^{l} z_i p(z_i) \quad (12)$$

Network parameters: Activation function is the sigmoid function given by the formula (13).

$$\sigma(\gamma) = \frac{1}{1+e^{-\gamma}} \quad (13)$$

Sigmoid function is a smooth switch function as shown by the curve of Figure 4. It has the property described by expression (14).

$$\sigma(\gamma) \to \begin{cases} 1 & as\ y \to +\infty \\ 0 & as\ y \to -\infty \end{cases} \quad (14)$$

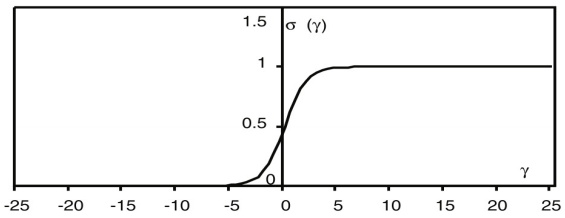

Figure 4. Sigmoid function.

Functioning of the proposed Technique: the designed classifier works like an automaton that traverses black skin lesion images and is able to differentiate healthy regions from lesions regions. So, when an image is input, the first step consists in dividing it into blocks of pixels of size 3x3. Then, features are calculated for each block and the equivalent function of the classifier is used to calculate the output. When the decision of the classifier is close to 1, all pixels values are replaced by 1. If, it's the contrary, values are replaced by 0. Thus, at the end we obtain a binary rebuilt image (cf. flowchart of figure 5).
The corresponding pseudocode of all this process is:

```
VARIABLES InputImage, F, Features[9], NbOfBlocks, Blocks[],OutputImage.
PREDEFINED FUNCTIONS CalcFeatures, ComputeNN, ExtractBlocks,
BEGIN
READ InputImage
DO [NbOfBlocks, Blocks] = ExtractBlocks(InputImage)
count = 0
WHILE count < NbOfBlocks
        count = count +1
        Features = CalcFeatures(Blocks(count))
        F=ComputeNN(Fetaures)
        If (0.5<F<=1) THEN
                Blocks(count)=1
        ELSE
                Blocks(count)=0
        ENDIF
ENDWHILE
WRITE OutputImage
END
```

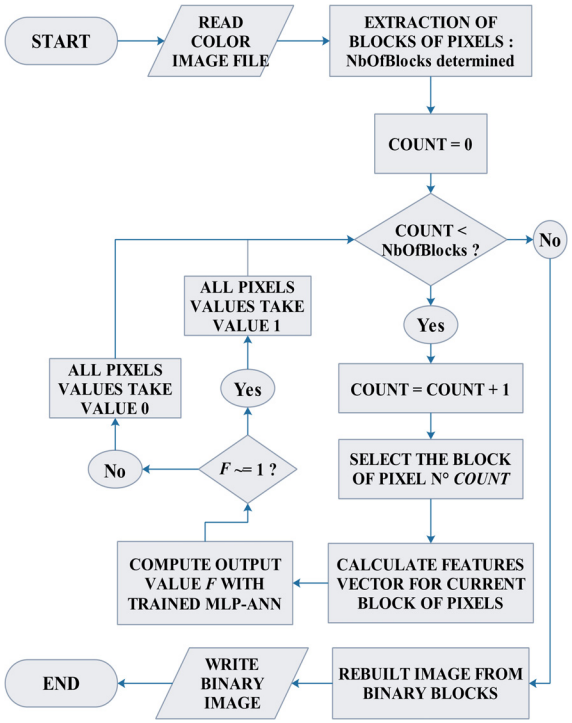

Figure 5. Flowchart of the proposed recognition technique

Evaluation metrics: We used six metrics to evaluate the performance of our classifier: Sensitivity, Specificity, Accuracy, False Positive Rate, Precision or Positive Predictive Value (PPV), Negative Predictive Value (NPV) and F1-Score. To define these metrics, let: TP (true positive) stand for the number of regions correctly classified as lesion region, TN (true negative) be the number of regions correctly classified as healthy regions, FP (false positive) the number of regions wrongfully classified as lesion and FN (false negative) be the number of regions classified as healthy but which are in reality lesion regions.

- Sensitivity or True Positive rate (TPR):

$$TPR = \frac{TP}{TP+FN} \times 100 \quad (15)$$

- False Positive Rate (FPR):

$$FPR = \frac{FP}{FP+TN} \times 100 \quad (16)$$

- Specificity (SPC) or True Negative Rate:

$$TPR = \frac{TN}{FP + TN} \times 100 \quad (17)$$

- Accuracy (ACC):

$$ACC = \frac{TP + TN}{TP + FN + FP + TN} \times 100 \quad (18)$$

- Precision or Positive Predictive Value (PPV):

$$PPV = \frac{TP}{FP + TP} \times 100 \quad (19)$$

- Negative Predictive Value (NPV):

$$NPV = \frac{TN}{FN + TN} \times 100 \quad (20)$$

4. Results and discussion

Results: We got best performances with six neurons in hidden layer. With this configuration, the network achieved his best validation performance after 457 iterations and the cross-entropy value of the objective function is around 0.083 (see Figure 6).

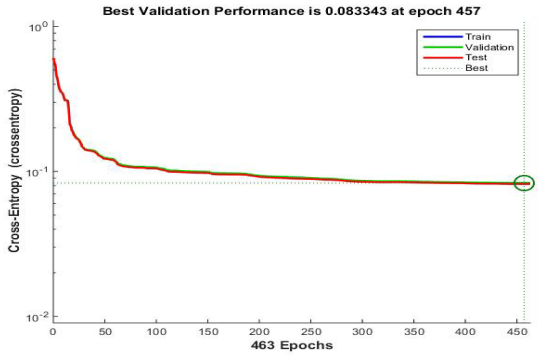

Figure 6. Training performance.

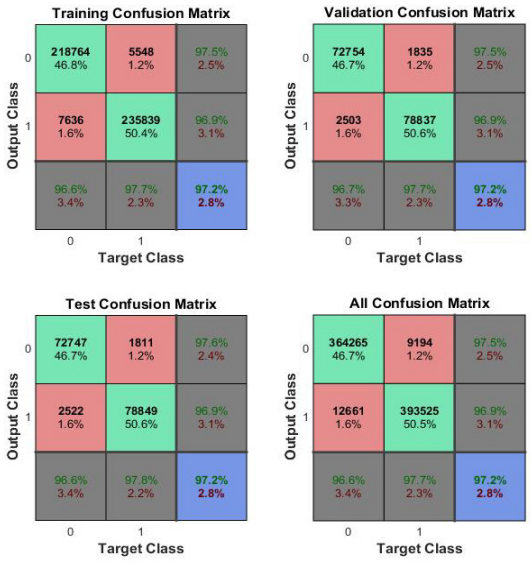

Figure 7. Confusion matrix.

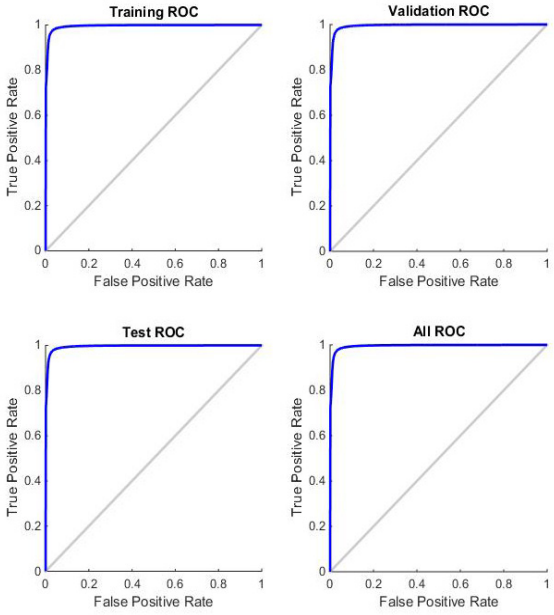

Figure 8. ROC Curves of the classifier.

The classification performance is good, considering error rates shown by confusion matrix of figure 7. Indeed, confusion matrix help to know percentages of samples which are misclassified in each set. According to the confusion matrix, the False Match Rate (FMR) in both training, validation and test stages is 2.8%. Moreover, the performance of the obtained classifier is more illustrated by the ROC curves of Figure 8. The form of ROC curve shows us that we have an excellent classifier if we refer to [32]. Indeed, the greater the area under the curve (AUROCC) is, the better the classifier is [33]. Finally, the values of evaluation metrics are reported in Table II.

Table II. Values of Evaluation Metrics

Metrics	Values
True Positive Rate (TPR) or Sensitivity	96,9%
True Negative Rate or Specificity (SPC)	97,5%
False Positive Rate (FPR)	2,5%
Precision or Predictive Positive Value (PPV)	97,7%
Negative Predictive Value (NPV)	96,6%
Accuracy (ACC)	97,2%

Discussion: In our modelling, 1s stand for normal or healthy skin region and 0s for lesion regions. Thus, we can notice that 3.1% of normal skin regions are misclassified; whereas only 2.5% of lesion regions are misclassified. These values are satisfactory since low error rate in classification of lesion regions is particularly important for future segmentation purpose.

The sensitivity of the classifier is: 96,9 %; its Specificity is: 97,5% and the False Positive Rate (FPR) is: 2,5%. These values are significant, though poor to validate machine learning experiments [32]. So, to strengthen our results, the following values are considered: Precision or PPV: 97,7%; NPV: 96,6%; and Accuracy: 97,2%. Their high values (more than 95%) indicate a certain reliability.

However, our results need to be compared with results obtained by similar work, although there is no specific previous work with black skin in the literature, apart from ours published in [8]. For this purpose, two works have caught our attention: those of (Madan et al., 2011) and (Jafari et al., 2016). The first worked on the detection of acne-like regions in macroscopic medical images of face [13]. The second recently used deep learning to extract skin lesions from non-dermoscopic (macroscopic) images [22]. A comparison with our results is made in Table III on obtained values for three metrics used by both authors: best results are bold.

Table III. Comparison of Detection performances in Macroscopic Skin Images

	Papers or Works		
Metrics	**Madan et al., 2011**	**Jafari et al., 2016**	**Our Work**
Sensitivity	90,4 %	95,2 %	**96,9 %**
Specificity	88 %	**98,8 %**	97,5 %
Accuracy	89,2 %	**98,5 %**	97,2 %

Best results of specificity and accuracy are obtained by Jafari et al., whereas best sensitivity value is obtained by us. This shows that our recognition performances need to be improved, even if the gap is not very big. However, it is important to note that both works compared to ours, were performed on white skin. This could justify the best performances. Indeed, contrasts between healthy regions and lesions are much sharper in this kind of skin.

5. Conclusion

The major contribution of this article arise from the use of ANN for black skin lesions. Indeed, using MLP-ANN for recognition tasks is not new but finding the good learning features to achieve good performances is the main contribution of this research work. The trained classifier identifies lesion-like regions in black skin medical images. To do this, we first set up a dataset of size around 800.000 examples. Texture and color features have been calculated for each of these examples. After that, we trained the network, while varying the number of neurons in hidden layer in order to get best performances. Finally we obtained a very good classifier which is able to differentiate lesion regions from safe skin regions in medical images with a small error rate.

This study also allowed us to highlight the differences between black skin and white skin. These differences exist firstly in terms of color, secondly in anatomical and structural terms. They induce difficulties to dermatology practitioners, as seen in publications made on the subject. Texture and color information used here as learning parameters, confirms practices of black skin specialists, who usually resort to skin palpation (searching texture changes) and observation of color changes to make their diagnostics.

But, although the performances of the obtained classifier are good, error rate is not less considerable. This is why the developed technique is used in "artifact detection" stage. Thus, further processing have to be made on resulting images before segmentation.

6. Acknowledgements

We would like to thank Doctor Hugues ADEGBIDI of Hubert Maga National University Hospital (CNHU HKM) of Cotonou (Benin) for his valuable help in this work.

7. References

[1] W. V. Stoecker, and R. H. Moss. Computerized Medical Imaging and Graphics. In Editorial: digital imaging in dermatology, 16(3), pp. 145–150. 1992.

[2] A. Amelio, and C. Pizzuti. Skin lesion image segmentation using a color genetic algorithm. In Proceedings of the 15th annual conference companion on Genetic and evolutionary computation, pp. 1471-1478. 2013.

[3] A. A. A. Al-abayechia, X. Guoa, W. H. Tana, and H. A. Jalabc. Automatic skin lesion segmentation with optimal colour channel from dermoscopic images. SCIENCEASIA, pp. 40, 1-7. 2014.

[4] A. Pennisi, D. Bloisi, D. Nardi, A. R. Giampetruzzi, C. Mondino, & A. Facchiano. Melanoma detection using Delaunay triangulation. In IEEE 2015 27th International Conference on Tools with Artificial Intelligence (ICTAI), pp. 791-798. 2015.

[5] M. E. Celebi, Q. Wen, S. Hwang, H. Iyatomi, and G. Schaefer. Lesion border detection in dermoscopy images using ensembles of thresholding methods. Skin Research and Technology, 19(1), pp. 252-258. 2013.

[6] G. S. Puigdemont, R. N. Sintes, and T. Dieng. Dermatology with black skin patients. Euromedice. 2008.

[7] D. Wallach. Specific aspects of dermatological diagnosis on black skin. In Rev. Pratt Review, pp. 3675-3688. 1981.

[8] G. Azehoun-Pazou, M. K. Assogba, and A. Vianou. A method of automatic black skin lesion's macroscopic image analysis. International Journal of Computer Applications & Information Technology, 4(1), pp. 9-14. 2013.

[9] P. Wighton, T. K. Lee, H. Lui, D. I. Mclean, S. M. Atkins. Generalizing Common Tasks in Automated Skin Lesion Diagnosis. IEEE Transactions on Information Technology in Biomedicine, 15(4). 2011.

[10] I. S. Akila, and V. Sumathi. Detection of Melanoma Skin Cancer using Segmentation and Classification Algorithm. In National Conference on Information and Communication Technologies (NCICT). 2015.

[11] P. Rubegni, G. Cevenini, M. Burroni, R. Perotti, G. Dell'Eva, P. Sbano, ... & L. Andreassi. Automated diagnosis of pigmented skin lesions. International Journal of Cancer, 101(6), pp. 576-580. 2002.

[12] V. H. Patil, D. S. Bormane, and V. S. Pawar. An automated computer aided breast cancer detection system. International Journal on Graphics, Vision and Image Processing, 6(1), pp. 69-72. (2006).

[13] S. K. Madan, K. J. Dana, & O. Cula. Learning-based detection of acne-like regions using time-lapse features. In 2011 IEEE Signal Processing in Medicine and Biology Symposium (SPMB), pp. 1-6. 2011.

[14] M. Egmont-Petersen, D. de Ridder, and H. Handels. Image processing with neural networks—a review. Pattern recognition, 35(10), pp. 2279-2301. 2002.
[15] N. K. Ragesh, A. R. Anil, & R. Rajesh. Digital image denoising in medical ultrasound images: a survey. In ICGST AIML 11th Conference, Dubai, UAE, 12, pp. 67 - 73. 2011.
[16] M. Yasmin, M. Sharif, and S. Mohsin. Neural networks in medical imaging applications: A survey. World Applied Sciences Journal, 22(1), pp. 85-96. 2013.
[17] A. Chaudhry, A. Khan, J. Y. Kim, and Q. Q. Niu. Intelligent Image Restoration Approach: Using Neural Networks to Eradicate Dilemma in Punctual Kriging. Life Science Journal, 10(1), pp. 1631-1641. 2013.
[18] R. H. Pugmire, R. M. Hodgson, and R.I. Chaplin. The properties and training of a neural network based universal window filter developed for image processing tasks. In S. Amari, N. Kasabov (Eds.), Brain-like computing and intelligent information systems, Springer-Verlag, Singapore, pp. 49–77. 1998.
[19] A. Chaudhry, A. Khan, A. M. Mirza, A. Ali, M. Hassan, and J. Y. Kim. Neuro fuzzy and punctual kriging based filter for image restoration. Applied Soft Computing, 13(2), pp. 817-832. 2013.
[20] A. J. Schofield, P. A. Mehta, T. J. Stonham. A system for counting people in video images using neural networks to identify the background scene, Pattern Recognition, 29 (8), pp. 1421–1428. 1996.
[21] R. Sammouda, J. A. Hassan, M. Sammouda, A. Al-Zuhairy, H. A. ElAbbas, Computer Aided Diagnosis System for Early Detection of Lung Cancer Using Chest Computer Tomography Images. In ICGST GVIP 5th Conference, Cairo, Egypt, pp. 1 - 8. 2005.
[22] M.H. Jafari, E. Nasr-Esfahani, N. Karimi, S. M. Soroushmehr, S. Samavi, & K. Najarian. Extraction of Skin Lesions from Non-Dermoscopic Images Using Deep Learning, arXiv preprint arXiv:1609.02374. 2016
[23] F. Amato, A. López, E. M. Peña-Méndez, P. Vaňhara, A. Hampl, and J. Havel. Artificial neural networks in medical diagnosis. Journal of applied biomedicine, 11(2), pp. 47-58. 2013.
[24] K. Korotov and R. Garcia. Computerized analysis of pigmented skin lesions: a review. 2012.
[25] G. Zhang, B. E. Patuwo, and M. Y. Hu. Forecasting with artificial neural networks: The state of the art. International journal of forecasting, 14(1), pp. 35-62. 1998.
[26] N. Karayiannis, and A. N. Venetsanopoulos. Artificial neural networks: learning algorithms, performance evaluation, and applications. Springer Science & Business Media, 209. 2013.
[27] W. S. McCulloch, and W. Pitts. A logical calculus of the ideas immanent in nervous activity. The bulletin of mathematical biophysics, 5(4), pp. 115-133. 1943.
[28] I. A. Basheer, and M. Hajmeer. Artificial neural networks: fundamentals, computing, design, and application. Journal of microbiological methods, 43(1), pp. 3-31. 2000.
[29] B. Müller, J. Reinhardt, and M. T. Strickland. Neural networks: an introduction. Springer Science & Business Media. 2012.
[30] G. Deco, and D. Obradovic. An information-theoretic approach to neural computing. Springer Science & Business Media. 2012.
[31] F. Wang, V. K. Devabhaktuni, C. Xi, and Q. J. Zhang. Neural network structures and training algorithms for RF and microwave applications. International Journal of RF and Microwave Computer-Aided Engineering, 9(3), pp. 216-240. 1999.
[32] T. Fawcett. ROC graphs: Notes and practical considerations for researchers. In Machine learning Journal, 31(1), pp. 1-38. 2004.
[33] K. H. Zou, A. J. O'Malley, and L. Mauri. Receiver-operating characteristic analysis for evaluating diagnostic tests and predictive models. Circulation, 115(5), pp. 654-657. 2007.

Biographies

Géraud Azehoun-Pazou received his Engineer degree in Informatics and Telecommunications in 2012 and the DEA degree "Diplôme d'Etudes Approfondies" in 2013 from the Polytechnic School of Abomey-Calavi, Benin. Currently he is a PhD student at University of Abomey-Calavi in the LETIA Laboratory under the supervision of Kokou Assogba. His research interests include Image processing, Artificial Intelligence, Object detection and tracking.

Dr. Kokou Assogba obtained his PhD degree in Images and Signal Processing in 1999 at University Paris XII Val de Marne, France. He is working, since as teacher-researcher in Computer Science and Electronics at University of Abomey-Calavi. He is Senior Member and recently became Head of the Laboratory of Electronics, Telecommunications and Applied Informatics (LETIA). His main research interests are: Digital Image processing, Pattern Recognition, Images Segmentation and smart technology.